10 Passive Cable Modeling

William R. Holmes

The application of passive cable theory to neuronal processes has a long and rich history (reviewed by Rall, 1977). Neuronal processes, being long and thin with an electrically conducting core surrounded by a membrane with high resistance, are naturally described as core conductors. Cable theory (named for its application to the first transatlantic telegraph cable) provides a straightforward means to study core conductors and has proved to be highly relevant and useful for the study of neuronal processes. Passive cable theory assumes that membrane properties are constant (independent of voltage and time). Although there is much evidence that membrane properties are not passive (see chapter 11), passive cable theory and passive cable modeling remain important for several reasons. First, they provide an intuition that is difficult to attain otherwise for understanding how neurons function; nonlinear properties are notoriously nonintuitive. Second, passive cable theory provides a number of significant insights whose usefulness carries over to the nonlinear case. Third, passive neuron models provide an important starting point or reference case from which one can build more complex models with excitable properties. Fourth, the propagation and summation of synaptic inputs are largely determined by passive properties. Finally, the effects that voltage-dependent conductances have on dendrites are heavily influenced by the passive electrotonic structure.

This chapter introduces basic passive cable theory. It describes properties of passive systems important for experimentalists and presents some insights from cable theory, many of which have received too little attention. It then discusses from a historical view how to estimate electrotonic parameter values from experimental data, along with problems associated with these older techniques. Finally, modern methods for estimating parameter values from data for passive systems and guidelines for constructing passive models are discussed, along with potential pitfalls that one should know. More detailed expositions and additional background on many of these topics are given in monographs by Jack et al. (1975), Koch (1999), Rall (1977), Rall et al. (1992), Rall and Agmon-Snir (1998), and Segev et al. (1994).

10.1 Electrotonic Parameters, the Cable Equation, and the Equivalent-Cylinder Model

To understand insights from cable theory, it is useful to review briefly some basic properties of neurons, show where the cable equation comes from, discuss some misconceptions about the meaning of some electrotonic parameters, and introduce the equivalent-cylinder model.

Membrane Potential and Input Resistance

There is a voltage difference across the neuron membrane resulting from the different distributions and membrane permeabilities of ions and charged molecules on either side of the membrane. This voltage difference across the membrane typically ranges from 40 to 90 mV among cell types, with the inside being negative relative to the outside. We say that cells have a resting membrane potential, V_m, of -40 to -90 mV. If we inject constant current into the cell, the voltage will change to a new steady-state value, illustrating another basic property of neurons, the input resistance, R_N. For passive systems, input resistance is computed simply from Ohm's law as $R_N = \Delta V/\Delta I$ where ΔV is the change in voltage that occurs with the change in applied current, ΔI. Input resistance is an important parameter to measure because it illustrates in a general way how excitable a cell is in response to synaptic input.

Input resistance, R_N, as a characteristic property of a cell, is measured at the soma. However, it is useful at times to refer to a local input resistance. This is the input resistance that would be measured at a dendritic location if an electrode could be placed there. Because dendritic processes are often very thin, local input resistance is typically larger than the input resistance measured at the soma (see section 10.2), but this is not necessarily the case.

Membrane Capacitance and Resistance

When a current is injected into a cell, the new steady-state voltage is not reached instantaneously. This can be explained by considering the properties of the membrane. The neuron membrane is a lipid bilayer of limited thickness and because the voltage inside is negative relative to the outside, the membrane stores and separates charges. We say the membrane has a capacitance. The amount of charge, Q, separated by a capacitor is given by the formula $Q = CV$ where C is the characteristic capacitance of the membrane and V is the voltage difference across the membrane. The specific membrane capacitance, C_m, for neurons has long been considered to be a biological constant (Cole, 1968) with a value of approximately 1.0 $\mu F/cm^2$. This value is based on measurements made from the squid axon (Curtis and Cole, 1938) and may be a slight overestimate. Squid axon has a high density of proteins that form voltage-dependent ion channels in the membrane. Artificial lipid bilayers with no

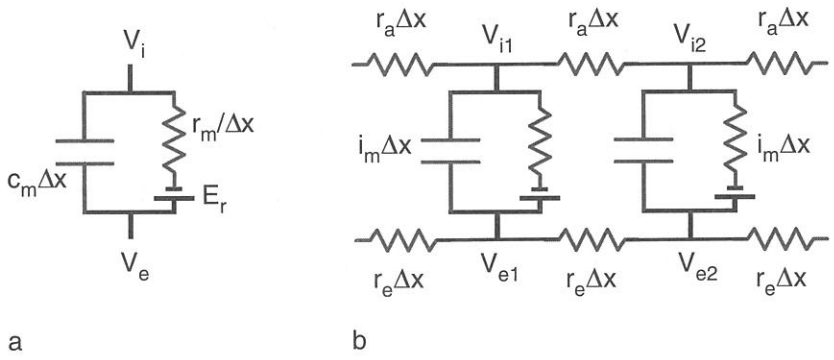

Figure 10.1
Conceptual models for neuronal membrane. (a) Simple circuit for a patch of membrane. (b) Circuit for a neuron cable. V_i is the intracellular voltage, V_e is the extracellular voltage, E_r is the membrane battery, r_m is the resistivity of a unit length of membrane (Ωcm), c_m is membrane capacitance per unit length (μF/cm), r_a (also called r_i) is axial resistivity per unit length of cable (Ω/cm), r_e is extracellular resistivity per unit length (Ω/cm) and Δx is the length of the patch. These are related to the specific units of measure described in the text by $r_m = R_m/\pi d$, $c_m = C_m \pi d$, $r_a = 4R_a/\pi d^2$, where d is the diameter of the cable.

embedded membrane proteins tend to have a lower C_m (Benz et al., 1975; Niles et al., 1988), with values ranging from 0.65 to 0.94 μF/cm^2, depending on the lipid composition and the thickness of the hydrocarbon core. More recently, Gentet et al. (2000) made direct measurements of C_m in cortical pyramidal, spinal cord, and hippocampal neurons and reported an average value of 0.9 μF/cm^2.

The lipid bilayer also provides a resistance to current flow. If the membrane were a pure lipid bilayer, the specific membrane resistivity, R_m, would be in the neighborhood of 10^8 Ωcm^2 (Almers, 1978) or higher (Hille, 2001). However, the membrane is studded with proteins, some of which form ion channels, and this reduces the membrane resistivity at rest to the 10^4–10^5 Ωcm^2 range. Given that the membrane has a capacitance and a resistance, it is natural to develop a conceptual model of the membrane as an electrical circuit as in figure 10.1a, where the battery, E_r, represents the membrane potential, and to consider membrane current as the sum of the current flows through the separate capacitive and resistive branches of this circuit.

Axial and Extracellular Resistance

The simple conceptual model of figure 10.1a applies for a patch of membrane or for spherical or isopotential cells, but neuronal processes more typically resemble cylinders or cables. In neuronal cables, current flows not only through the capacitance and resistance of the membrane, but also through the interior of the cell and in the extracellular space as well. When these factors are considered, our conceptual model of the neuron cable becomes the electric circuit shown in figure 10.1b. Strictly speaking, there is three-dimensional current flow inside the neuronal cable, but in practice

we consider only the longitudinal current down the cable through the axial resistance provided by the intracellular medium. This is reasonable because the process diameter is generally small, making intracellular resistance to radial current flow negligible compared with the membrane resistance; similarly, we also neglect intracellular resistance to angular current flow.

The specific intracellular or axial resistivity, R_a, is a difficult parameter to measure (see discussion in Rall et al., 1992). Intracellular resistivity is traditionally labeled R_i. Unfortunately some papers incorrectly use R_i to mean input resistance. To remove all ambiguity, we use R_a for intracellular or axial resistivity and R_N for input resistance. Estimates for R_a range from 50 to 400 Ωcm in mammalian neurons; lower estimates have been obtained in marine invertebrates where the intracellular ion concentrations are much different. For example, the resistivity of "Woods Hole seawater" is 20 Ωcm and the resistivity of squid axoplasm, measured relative to seawater, is 1.0–1.6 times higher (Cole, 1975; Carpenter et al., 1975). By comparison, at 20 °C, mammalian saline has an R_a of 60 Ωcm and frog Ringer's solution has an R_a of 80 Ωcm (Hille, 2001). Barrett and Crill (1974) measured an average R_a of 70 Ωcm in cat motoneurons at 37 °C. Values of 100–250 Ωcm have been reported for red blood cells and frog skeletal muscle (Pilwat and Zimmerman, 1985; Schanne and De Ceretti, 1971). Clements and Redman (1989) computed a value of 43 Ωcm at 37 °C for motoneuron cytoplasm based on ion composition, but noted that the actual R_a will be higher than expected from known concentrations of ions and ion mobility because of the presence of charge binding and various proteins, carbohydrates, and organelles. Different intracellular compositions may explain the variability in measured values for the same cell type as well as that among different cell types. Other factors affecting R_a are the composition of the extracellular medium (Schanne, 1969; the mechanism is unclear; it may be because of an induced change in the free and bound concentrations of ions inside) and temperature (R_a will decrease with increasing temperature; Trevelyan and Jack, 2002).

Extracellular resistance is usually assumed to be negligible in models. While this is clearly not true (because extracellular recordings could not be made otherwise and ephaptic coupling has been observed among tightly packed neurons; Jefferys, 1995), it is a reasonable assumption in most situations when the extracellular space is large (e.g., see Rall, 1959), the neuron is isolated, or the concern of the model is a single neuron.

Converting the Conceptual Model to the Cable Equation

The conceptual models represented in figure 10.1 can be converted into mathematical equations by straightforward application of Ohm's law, $Q = CV$, and Kirchoff's law (conservation of current at a node). The most difficult part of this conversion is to keep track of the units of the various parameters. The mathematical equations for the conceptual models in figure 10.1 are

$$i_m = c_m \frac{dV}{dt} + \frac{V}{r_m}, \tag{10.1}$$

which says the membrane current equals the sum of the capacitive and resistive currents across the membrane and

$$\frac{1}{r_a}\frac{\partial^2 V}{\partial x^2} = c_m \frac{\partial V}{\partial t} + \frac{V}{r_m}, \tag{10.2}$$

which says the change (or difference) in intracellular current flowing along the inside of the cable equals the current that flows across the membrane. Equation (10.2) is usually multiplied by r_m and rearranged to yield the cable equation

$$\tau \frac{\partial V}{\partial t} = \lambda^2 \frac{\partial^2 V}{\partial x^2} - V, \tag{10.3}$$

where τ is the membrane time constant and λ is the space constant defined by

$$\tau = r_m c_m = R_m C_m \quad \lambda = \sqrt{\frac{r_m}{r_a}} = \sqrt{\frac{R_m d}{4R_a}}. \tag{10.4}$$

(See figure 10.1 caption for notation definitions.) Note that if extracellular resistance is included in the derivation, then $r_a + r_e$ is substituted for r_a in the definition of λ. Equation (10.3) is often expressed in nondimensional form by defining $T = t/\tau$ and $X = x/\lambda$ to get rid of those pesky constants and allow a more straightforward mathematical analysis. Other useful terms are L, the electrotonic length, which is defined by $L = \ell/\lambda$ where ℓ is the physical length of the cable; and the electrotonic distance X, defined as earlier by $X = x/\lambda$, the physical distance from the beginning of the cable divided by the space constant. The parameter L will appear numerous times in the following discussion.

Misconceptions about τ and λ

Equation (10.1) and the steady-state version of equation (10.3) (left-hand side = 0) are easily solved and the solutions are often used in textbooks to indicate the importance of τ and λ for electrical signaling. However, this is often done in a misleading way. A solution for equation (10.1) is $V(t) = V_0 e^{-t/\tau}$, from which it is usually concluded that τ is the time it takes for a voltage perturbation to decay from rest to 37% $(1/e)$ of its initial value. However, rarely is it stressed that this is true only for an isopotential cell or sphere (the conditions leading to equation 10.1). For cylinders, the decay (as well as charging) is much faster (figure 10.2a). In an infinite cylinder, voltage will be only 16% of its initial value at time $t = \tau$, and in a finite cable with an electrotonic length $L = 1.0$, voltage will decay to 28% of its initial value in this

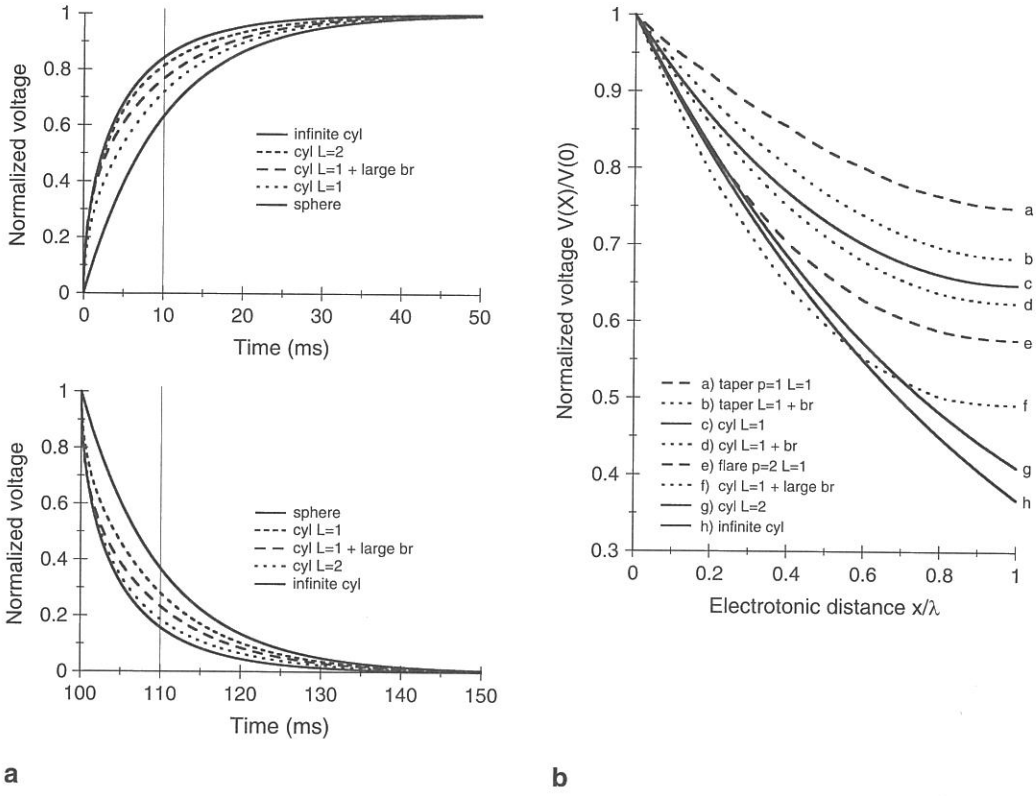

Figure 10.2
Effect of geometry and boundary conditions on transient and steady-state voltage changes. (a) A constant current is applied at time $t = 0$ ms for 100 ms. The upper curves show the voltage during the first 50 ms of the charging phase and the lower curves show the voltage decay for the first 50 ms after the current is terminated. Note the symmetry of the charging and decay transients. Curves top to bottom are in the same order as in the legends and represent the responses in an infinite cylinder, a sphere, finite cylinders with electrotonic lengths of 1 and 2, and a cylinder with an electrotonic length of 1 with a large side branch attached. The vertical lines at 10 and 110 ms are times $t = \tau$ after the current injection is turned on or off ($\tau = 10$ ms). (b) Steady-state voltage decay with distance. Geometries include cylinders with thick (f) and thin (b, d) side branches. Cases with flare (e) and taper (a) were constructed with symmetric trees with diameters of parent and daughter branches satisfying $(d_{\text{parent}})^p = \sum(d_{\text{daughters}})^p$ at branch points where $p = 2$ represents flare and $p = 1$ represents taper. Electrotonic length was 1.0 in all cases except (g) and (h).

time. In a finite cylinder, there are additional, faster equalizing time constants that increase the rate of the decay. These are described in more detail later. In figure 10.2a the charging transients are also shown. It is not readily appreciated by those new to the field that charging and decay transients are symmetric.

Similarly, a steady-state solution for equation (10.3) is $V(x) = V_0 e^{-x/\lambda}$, from which it is usually concluded that λ is the distance at which the steady-state voltage decays to 37% $(1/e)$ of its value at the origin. However, rarely is it stressed that the solution and the conclusion are valid only for an infinitely long cable. For a finite cable with an electrotonic length $L = 1.0$, voltage will decay to only 65% of its value at the origin at a distance $x = \lambda$. Differences such as this arise because of the boundary conditions at $x = \lambda$. In the infinite-cylinder case, an infinite cylinder with its associated conductance is attached to the (artificial) boundary at $x = \lambda$ and current flows into this cylinder, whereas in a finite cylinder with $L = 1.0$, the cylinder ends at $x = \lambda$. For a sealed-end boundary condition, there is no conductance and no current flow at this boundary (assuming a leaky end through a small end cap of a membrane makes a negligible difference). Voltage decay with distance is also affected by taper or flare in the diameter of the equivalent cable and by side branches off the main cable. Examples of this are shown in figure 10.2b.

Nevertheless, τ remains a useful measure of voltage decay with time and λ remains a useful measure of voltage decay with distance. However, it is important to understand how boundary conditions and complex dendritic geometry can influence temporal and spatial voltage summation and voltage decay in a neuron.

Equivalent-Cylinder Model

Although neurons are highly branched structures rather than single cylinders, a highly branched neuron can be equivalent mathematically to a single cylinder when a particular set of conditions holds. This is Rall's equivalent-cylinder model (Rall 1962a,b). Starting with the most distal branches and working inward, each pair of daughter branches is replaced by a single cylinder having the same input conductance and electrotonic length as the two daughter branches but having the same diameter as the parent branch. This is possible when R_m and R_a are uniform; all terminal branches have the same distal boundary condition (e.g., no current through the end of the branch); all terminals end at the same electrotonic distance from the soma; and the daughter branch diameters raised to the 3/2 power and summed equal the parent branch diameter raised to the 3/2 power (often called the 3/2 rule or 3/2 power law). These constraints also preserve input conductance and membrane area between the branched tree and the equivalent cylinder.

The equivalent-cylinder model is a useful construct for studying the effect of current input or a voltage clamp applied at the soma on voltage changes throughout the dendritic tree. Its simplicity allows mathematical analysis and ready insight into

dendritic function. However, it is less useful for studying dendritic input. Any input to a location in the equivalent cylinder would have to be divided among all dendrites in the fully branched structure at the same electrotonic distance for the responses to be the same. The equivalent-cylinder model is also useful for estimating parameter values, as discussed later. Clearly no dendritic tree is likely to satisfy all of the constraints of the equivalent-cylinder model, particularly the constraint of all dendrites terminating at the same electrotonic distance from the soma. A number of neurons seem to follow the 3/2 rule over much of their dendritic trees (Barrett and Crill, 1974; Turner and Schwartzkroin, 1980; Durand et al., 1983) but others do not (Larkman et al., 1992).

10.2 Properties of Passive Systems

To model complex branching structures, one can apply the cable equation (equation 10.3) to every unbranched segment of the dendritic tree and then match boundary conditions (conservation of current, continuity of voltage) at the branch points. While there are straightforward ways to do this analytically for the steady-state case, the mathematics quickly becomes very messy and complicated for the transient or time-dependent solution. A simplification is to make unbranched segments small enough so that they are essentially isopotential, model the membrane current of these segments with equation (10.1), and then couple adjacent segments with "coupling resistances" based on segment axial resistances (see chapter 11, section 1). This is the compartmental modeling approach, and although it is simpler because the system of partial differential equations is reduced to a system of ordinary differential equations, the mathematics again becomes messy very quickly. It is much more convenient to model complex branching structures numerically, and there are many freely available software packages, such as NEURON and GENESIS (see the software appendix), for doing this. Because passive models only require morphology, R_m, R_a, and C_m, they are solved particularly quickly with these software programs and model results can then be compared with data from experimental cells whose voltage responses have been made passive through the use of pharmacological blockers.

Linearity (and Nonlinearity)

A key property of a passive system is its linear response to current injection. Input resistance can be calculated from any single constant current injection because Ohm's law applies. Doubling the current will double the size of the voltage response, leaving the input resistance value unchanged. Perhaps less intuitive is the fact that if current is injected in two different places in the cell, the voltage response at any location (both transient and steady state) will equal the sum of the voltage responses to the individual current injections applied separately. However, a passive system is

not linear when it comes to synaptic inputs. Synaptic currents can be modeled as $g_{syn}(V - E_{syn})$ or a synaptic conductance times a driving force (see chapter 6, section 6.1). If g_{syn} is doubled, the voltage response is not doubled because the driving force is reduced as the voltage approaches the synaptic reversal potential E_{syn}.

Reciprocity

Passive systems exhibit a nonintuitive symmetry in voltage responses called reciprocity (see discussion in Major et al., 1993b). The voltage response at the soma to current injection at a dendritic location will equal the voltage response at this dendritic location following the same current injection at the soma. It should be noted that the voltage responses at the injection sites and the degree of voltage attenuation between the injection site and the recording site may be drastically different, but the responses at the recording sites will be identical (e.g., figure 1 of Roth and Häusser, 2001). Checking for reciprocity is a good way to determine if a dendritic tree is passive or if blockers have been successful at making it so.

Asymmetric Voltage Attenuation

One property of passive systems discovered early on is the highly asymmetric voltage attenuation from a distal dendrite to the soma compared with voltage attenuation in the reverse direction. We first consider the case where a constant current is injected at the end of a distal dendrite. Because this terminal process is thin, axial current flow is relatively small (r_a is large) and therefore the input resistance at this location is large, producing a large voltage change. However, the steady-state voltage attenuation from the point of current injection to the first branch point will be substantial. At the branch point, current can continue to travel proximally toward the soma or else travel distally in the sibling branch. Because of the sealed-end boundary condition at the end of the sibling branch and the comparatively open-end boundary condition in the proximal direction, very little current goes in the distal direction, and as a consequence there is little voltage attenuation in the distal direction. Voltage attenuation from this branch point to the next proximal branch point is again substantial, while voltage attenuation in the distal direction in the sibling branch is again small as a consequence of the sealed-end boundary condition at the end of this distal path compared with the wide-open end in the proximal direction. This pattern is repeated as the current spreads proximally (Rall and Rinzel, 1973). Conversely, if the same current is injected at the soma, the local voltage change at the soma is relatively small because of the lower input resistance there, but voltage attenuation in the distal direction is limited because the current divides among multiple branches, with each terminal branch having a sealed-end boundary condition.

Voltage attenuation from a distal site to the soma for transient inputs can be orders of magnitude more severe than that for steady-state inputs. This fact raises

the question of whether brief distal synaptic inputs can play any role in exciting a cell. Despite the significant attenuation of the peak voltage from a distal site to the soma following a transient distal current input, the time course of the voltage response is much elongated at the soma, and the attenuation of the area of the voltage waveform (integral of the voltage over time) will only be as severe as the steady-state voltage attenuation discussed earlier. This is true regardless of the time course of the transient input in a passive system. Numerical examples of this are given in Rall and Rinzel (1973) and Rinzel and Rall (1974) for dendritic trees equivalent to a cylinder and in London et al. (1999) when R_m is nonuniform. More recent examples applied to morphological reconstructions of cortical and hippocampal neurons are given by Zador et al. (1995) and Carnevale et al. (1997). These studies use the log of voltage attenuation as the basis for a *morphoelectrotonic transform* that allows one to visualize voltage attenuation between any point in a dendritic tree and the soma (or attenuation in the reverse direction) to gain an intuitive appreciation of the functional structure of the cell.

10.3 Insights from Passive Cable Theory

Consequences for Voltage Clamp

The voltage attenuation properties of passive systems have particular significance for the extent of a space clamp in the dendrites when the soma is voltage clamped. Although voltage attenuation from the soma to the distal tips is much less than the voltage attenuation in the reverse direction, the amount of attenuation is still significant. For example, suppose a cell with resting potential of -70 mV is approximated as an equivalent cylinder with electrotonic length $L = 1.0$ and the soma end is voltage clamped to -10 mV. Then the distal tips would be clamped to $-70 + 60/\cosh(L) = -31$ mV. Passive cable theory allows one to estimate the space-clamp error for a given voltage clamp at the soma, and suggests that this error can be quite significant (Johnston and Brown, 1983; Rall and Segev, 1985; Spruston et al., 1993). One consequence of this is that synaptic reversal potentials can be estimated accurately in a voltage-clamp experiment only when the synapse is very close to the soma (Johnston and Brown, 1983; but see Hausser and Roth, 1997b). Suppose one is able to insert a voltage-clamp electrode into a dendrite. Because voltage attenuation from a distal branch toward the soma is much more severe than in the reverse direction, the extent of the space clamp in the dendrite would be extremely limited.

Consequences for the Placement of Inhibition and Excitation

The asymmetry of voltage attenuation also provides insight into why inhibition is typically located at the soma whereas excitation is typically located more distally.

Inhibition is very effective when placed at the soma because its effect will be felt throughout the cell without severe attenuation. Inhibition in distal dendrites is effective for shunting local excitation, but its effect is limited spatially (Rall, 1964, 1967; Koch et al., 1983; Segev and Parnas, 1983). As for excitation, excitatory input at the soma will not produce the large local voltage changes that occur with distal input. Although large local voltage changes with distal input will attenuate severely along the path to the soma in a passive system, they are apt to activate voltage-gated conductances in a nonpassive system. This suggests that perhaps excitation is better placed in the dendrites than at the soma, where local voltage changes would be smaller and less able to activate voltage-dependent sodium or calcium conductances.

Dendritic Filtering of Synaptic Inputs

Electrotonic parameters affect the amplitude and time course of the voltage response to synaptic inputs at the input location, but how important individual parameters are depends on whether the synaptic currents are brief or prolonged. If a synaptic input is brief, the rise time and perhaps the initial decay of the local voltage response are determined primarily by the time course of the synaptic conductance change, with the peak amplitude influenced by C_m, R_a, and the dendritic diameter, but not by R_m (Major et al., 1993a). The synaptic current will initially charge the local capacitance, start to flow longitudinally through the axial resistance, and only then will it begin to flow significantly through the membrane resistance. When the synaptic current ends, the initial local voltage decay is much faster than would be predicted from the membrane time constant. Only the late portion of the voltage decay is governed by τ_m. If synaptic currents are more prolonged, the peak local voltage response is determined by the local input resistance, which depends on R_m and R_a, but not C_m.

In passive systems, the dendrites provide a low-pass filtering of the voltage response to synaptic currents and here R_m plays an important role. Membrane resistivity will affect voltage attenuation through its influence on the space constant λ and will affect the time course of the voltage decay through its influence on τ. As the signal proceeds toward the soma, the voltage response is attenuated and becomes spread out. The time to peak and half-width of the voltage response at the soma can be used to predict how far a synapse is from the soma, with more distal inputs having a longer time to peak and a longer half-width (Rall, 1967). However, both time to peak and half-width are influenced by the synaptic conductance time course, electrotonic distance, the prevalence of side branches along the path to the soma and whether inputs are restricted to a single location; these factors make predictions of synaptic location with this method less precise (Iansek and Redman, 1973; Johnston and Brown, 1983; Redman and Walmsley, 1983; Bekkers and Stevens, 1996; Mennerick et al., 1995).

Propagation Velocity

Although mathematical expressions have been derived with various assumptions to describe the propagation velocity of a signal (Jack et al., 1975; Agmon-Snir and Segev, 1993), an intuitive way to think about propagation velocity is simply to consider velocity as distance divided by time where distance is represented by the space constant λ and time is represented by the time constant τ. If we do this, we find that velocity is proportional to $[d/(R_a R_m C_m^2)]^{1/2}$ and this expression clearly illustrates the dependence of velocity on electrotonic parameters and diameter.

Optimal Diameter

Can a neuron optimize the effectiveness of distal synaptic inputs by adjusting its morphological or electrotonic properties? The answer, perhaps surprisingly, is yes. Suppose a cell is represented by a cylinder 1,000 μm long. If current is injected into one end of the cylinder, can we choose electrotonic parameters to maximize the voltage at the other end? Clearly, voltage could be maximized if $R_m \to \infty$ or $R_a \to 0$, but what if R_m and R_a are fixed to finite and nonzero values? Then it turns out that voltage at the other end of the cylinder can be maximized for a particular choice of diameter.

The reason that an optimal diameter exists is that the effectiveness of an input will depend on its amplitude at the input site and the voltage attenuation to the soma. For a fixed length cable, if the diameter is large, then input resistance is low; an input will produce a small voltage response that will attenuate very little down the cable. If diameter is small, then input resistance is large; an input will produce a large voltage response that will attenuate considerably down the cable. There is an optimal diameter that will balance the competing forces of input resistance and attenuation on the voltage response. For a constant current input, the optimal diameter should be chosen to make the electrotonic length of the cable $L \approx 3$ (Holmes, 1989). Because of reciprocity in a linear system, diameters that maximize the voltage at a distal tip for current input at the soma will also maximize the voltage at the soma for current input at the distal tip. If the input is a synaptic input, particularly a transient synaptic input, the optimal diameter occurs for much smaller values of L. However, reciprocity does not hold for synaptic inputs because of the nonlinear effect of the driving force, and this means that diameters cannot be optimal for signaling in both directions. This analysis in a passive system suggests that it is possible that the morphology of a cell may be optimized to maximize the effectiveness of synaptic inputs from a given location having a particular time course (Mouchet and Yelnik, 2004; Ermi et al., 2001). A similar analysis has been done recently regarding optimal diameters for the placement of gap junctions (Nadim and Golowasch, 2006).

Branching Effects on Current Flow and the "3/2 Rule"

While the 3/2 rule is useful for reducing complex trees to an equivalent cylinder, it is less clear what use such a branching pattern might have in nature. It is tempting to suggest that the 3/2 rule might provide optimal diameters to maximize the effectiveness of certain inputs, but currently there is no evidence for this. One might ask if the 3/2 rule is the most efficient means to distribute voltage across branch points or wonder what happens to voltage drops at branch points when diameters do not follow this rule. Suppose diameters satisfy a different power rule at branch points. Suppose the power p equals 1 (taper) or 2 (flare). What effect does this have?

If diameters satisfy the 3/2 rule, there is impedance matching at branch points and this will be lost if $p \neq 3/2$. The result is that voltage attenuation away from the soma will change abruptly at branch points. If $p = 1$, voltage attenuation will be less steep before the branch point than after it. If $p = 2$, voltage attenuation will be steeper before the branch point than after it. Such changes are difficult to see clearly in plots (figure 10.2b) without larger deviations from the 3/2 rule, but they could have implications for how strongly somatic inputs are felt in proximal regions compared with distal regions. Conversely, for an input at the tip of a distal branch, there will always be an abrupt change in the rate of steady-state voltage attenuation at the branch point (see figure 4 of Rall and Rinzel, 1973). Attenuation will always be more shallow proximal to the branch point as current flows from the distal branch into a thicker proximal process and a sibling branch, but this attenuation between branch points is steeper if $p = 1$ and more shallow if $p = 2$ compared with when $p = 3/2$.

The result of this is that the asymmetry in steady-state voltage attenuation from a distal dendrite toward the soma compared with attenuation in the reverse direction is increased when $p = 1$ and reduced when $p = 2$ compared with the case where $p = 3/2$. Changes in attenuation are also accompanied by changes in input resistance, with R_N increased when $p = 1$ and reduced when $p = 2$. Because of the competing roles of input resistance and attenuation for determining optimal diameters, as mentioned earlier, it is possible that differences in the value of p may reflect a difference in how inputs in different parts of the dendritic tree are weighted.

Dendritic Spines

Passive cable theory has several implications for the function of dendritic spines (see Rall, 1974, 1978 and the review by Shepherd, 1996) and we will only mention two. First, spines provide a particular case of asymmetric voltage attenuation described earlier. There may be considerable voltage attenuation from the spine head to the dendrite if the spine stem resistance is large. However, there is virtually no voltage attenuation in the reverse direction; any voltage change in the dendrite is felt in the

spine. This fact ruled out an early hypothesis for spine function: that spines exist to isolate inputs from each other electrically. Second, an input on a spine is less effective than an identical input on the dendrite. Although this is true for passive models, it may not be true if voltage-dependent conductances are activated in spines.

10.4 Estimating Electrotonic Parameters—Historical View

To make passive models of neurons, it is essential to have estimates for the values of the electrotonic parameters as well as some representation for cell morphology. The electrotonic parameter whose value is known with the most certainty is C_m. Cole (1968) called C_m a biological constant with a value of approximately 1.0 $\mu F/cm^2$ and although this value is often used, it may be an overestimate, as discussed earlier. Axial resistivity, R_a, has been difficult to measure, but at least we believe we have good bounds for this parameter. However, values for R_m and a suitable morphology are more difficult to determine. Rall pioneered methods to estimate these parameters with the equivalent-cylinder model and we briefly review these.

Use of Time Constants to Estimate Electrotonic Parameter Values

Rall (1969) showed that the voltage response following the termination of a brief or sustained current input could be described mathematically as an infinite sum of exponential terms:

$$V = C_0 e^{-t/\tau_0} + C_1 e^{-t/\tau_1} + \cdots \tag{10.5}$$

If values for τ_0 and τ_1 can be estimated from a voltage transient by curve fitting or (in those days) "exponential peeling," then critical information about the cell can be obtained. First, τ_0, being the longest time constant, is equal to the membrane time constant τ_m. Because $\tau_m = R_m C_m$, we can estimate R_m assuming that C_m is 1.0 $\mu F/cm^2$. Second, Rall showed that if the cell can be approximated as an equivalent cylinder, then the electrotonic length of the cell can be estimated from the equation, $L = \pi/(\tau_0/\tau_1 - 1)^{1/2}$.

Although Rall derived several other formulas for L that involved use of the coefficients C_i and voltage-clamp time constants, this particular formula was the most widely used because the current clamp time constants were the easiest to obtain with confidence. With estimates of R_m and L, one could construct a simplified model of a cell in which it was not essential to have precise lengths and diameters of neuron processes as long as these values met the constraint of the estimated L value. Application of the Rall formula has provided substantial insight into the electrotonic structure of numerous types of neurons in scores, if not hundreds, of studies through the years (e.g., Nelson and Lux, 1970; Lux et al., 1970; Burke and ten Bruggencate,

1971; T. H. Brown et al., 1981a,b; Johnston, 1981; Stafstrom et al., 1984; Fleshman et al., 1988; Pongracz et al., 1991; Rapp et al., 1994; London et al., 1999).

What Do the Time Constants Represent?

In a cylinder, the time constant τ_1 represents an equalization of charge between the soma end of the cylinder and the distal end. Subsequent time constants represent additional harmonics of charge equalization between the two ends of the cylinder. It is this charge equalization that makes voltage decay (and voltage charging) initially faster in a cylinder than in an isopotential sphere, as mentioned briefly earlier. The τ_1 will be half the size of τ_0 for $L \sim 3$, one-tenth of τ_0 for $L \sim 1$, and one-hundredth of τ_0 for $L \sim 0.3$, so charge equalization will modify the voltage transient in all but the most electrotonically compact cells.

The advent of neuron reconstruction methods (chapter 8) has allowed modelers to use actual cell morphology in models, but for morphologies different from those of an equivalent cylinder, the time constants have a different meaning. In a compartmental model with N compartments, N time constants can be computed from the eigenvalues of the compartmental model matrix (the matrix $\mathbf{A}$ in the representation $dV/dt = \mathbf{A}V + \mathbf{B}$). It turns out that τ_1 represents charge equalization between the longest tip-to-tip path in the neuron, τ_2 represents charge equalization between the second longest tip-to-tip path, etc. These time constants are associated with odd eigenfunctions (having odd or $+/-$ symmetry with respect to the soma). Eventually there is a time constant, τ_{even}, associated with an even eigenfunction (even symmetry) with respect to the soma that represents charge equalization between a proximal membrane and a distal membrane. In a morphology represented by an equivalent cylinder, the coefficients of the time constants associated with odd eigenfunctions (τ_1, τ_2, etc.) are all equal to zero and the first time constant that appears with a nonzero coefficient after τ_0 is τ_{even}. However, if the morphology deviates from an equivalent cylinder, then these other time constants will not have zero coefficients. In neurons having terminations at different electrotonic lengths, such as pyramidal cells (apical versus basilar dendrites), some of these coefficients can be significant. The assumption made when applying the Rall formula is that the fitted τ_1 (sometimes called $\tau_{1\text{peel}}$) will equal τ_{even}, but this may not be the case if other time constants have significantly nonzero coefficients because the fitted τ_1 will most likely reflect the average of dozens of closely spaced time constants (W. R. Holmes et al., 1992).

Constructing Models from Morphology, τ_0 and R_N

Some labs began to apply the Rall methods after obtaining morphological and electrophysiological data from the same cell (e.g., Clements and Redman, 1989; Fleshman et al., 1988; Nitzan et al., 1990). Standard estimates of C_m and R_a, an estimate of R_m from the experimentally determined τ_0, plus the reconstructed morphology

should in theory provide all that is needed to construct passive models of these cells. However, when this was done in practice, some discrepancies were quickly noted. In particular, the input resistance, R_N, measured experimentally did not agree with the input resistance value calculated with the model.

Three hypotheses were proposed to explain these discrepancies. First, perhaps the standard values assumed for C_m and R_a were not correct. However, the changes required were too large for this possibility to be readily accepted. Second, perhaps the electrotonic parameters, in particular R_m, were not uniform in the cell. Unfortunately not enough information was available to distinguish among various R_m distributions. Third, it is well known that membrane does not necessarily provide a tight seal around intracellular electrodes, and perhaps an electrode shunt could cause an artificially low τ_0. The data seemed to be most consistent with this third possibility. This required estimation of an additional parameter, the soma shunt (Rose and Dagum, 1988; Rose and Vanner, 1988; Clements and Redman, 1989; Pongracz et al., 1991). Given that sharp electrodes introduce an artificial shunt at the soma, it became clear that earlier estimates of L obtained with the Rall formula overestimated the actual L by a factor of two in electrotonically compact cells and by 0–20% in electrotonically long cells (Holmes and Rall, 1992a). Furthermore, estimation of C_m, R_a, R_m, and the soma shunt cannot be done uniquely without accurate morphological and electrophysiological information from the same cell (W. R. Holmes and Rall, 1992b; Major et al., 1993a) and even then, it is possible to obtain several sets of parameter values that appear to fit the data equally well (Rapp et al., 1994).

Whole-Cell Patch Recordings

The development of the whole-cell patch-clamp technique allows one to avoid introducing an artificial shunt into the cell, but this recording method is not without its own issues. The technique may dialyze the cell, so it is important to have the appropriate medium composition in the electrode. In some of the early whole-cell patch data, values of input resistance and associated estimates of R_m and R_a were 5–10 times larger than estimates obtained with sharp electrodes. The reasons for this were that many of these recordings were done from immature neurons from young animals and the technique allowed more recordings from smaller cells to be successful; however, the biggest problem appears to have been cell dialysis. The use of the perforated-patch technique, along with better knowledge of what needs to go into the patch electrode (Kay, 1992), has brought estimates of these parameters back down substantially, although values remain higher than those obtained with intracellular electrodes (Pongracz et al., 1991; Spruston and Johnston, 1992; Staley et al., 1992). The use of whole-cell patch recordings has brought to light a fourth explanation of the discrepancies noted earlier that was known but largely ignored at the time—the accuracy of the morphological reconstructions. This is discussed further later.

10.5 Estimating Electrotonic Parameters—Recent Approaches

Recent efforts to estimate passive electrotonic parameters use whole-cell patch or perforated-patch recordings combined with morphological reconstructions from the same cell. A sample of these efforts for seven different cell types is discussed here. Patch recordings eliminate the soma shunt problem and this, together with complete morphological information from the same cell, removes a major source of non-uniqueness of parameter value estimates. After the experience with soma shunt caused by sharp electrodes, particular concern has been devoted to minimizing technical problems during experiments, such as those caused by electrode resistance and capacitance, and these are discussed at length in Major et al. (1994) and Roth and Hausser (2001).

The types of recordings that have been used in recent analyses are the response at the soma to a brief pulse of current (Thurbon et al., 1998; Roth and Hausser, 2001; Major et al., 1994; Trevelyan and Jack, 2002), short and long hyperpolarizing current pulses (Stuart and Spruston, 1998; Golding et al., 2005), or just long hyperpolarizing pulses (Chitwood et al., 1999). Brief pulses are presumed to be too brief to activate voltage-dependent conductances, leaving only a passive response for analysis. Responses to long hyperpolarizing pulses are typically done with H-channel blockers to linearize responses as necessary.

The morphological reconstructions were used to construct models and then parameter values for R_m, R_a, and C_m were fit in the models to match the voltage responses. Roth and Hausser (2001), Stuart and Spruston (1998), Golding et al. (2005) and Chitwood et al. (1998) used the multiple-run fitter in NEURON to do their fits, while other groups used direct fits with standard optimization methods. Three groups (Stuart and Spruston, 1998; Roth and Hausser, 2001; Golding et al., 2005) were able to record simultaneously from dendrites and the soma. Having recordings from multiple locations in the cell is exceptionally useful for fitting R_a and for determining whether R_m is uniform. Stuart and Spruston (1998) and Golding et al. (2005) could not find good fits to both dendritic and somatic recordings when R_m was assumed to be uniform; the fitted model responses decayed too slowly in the dendrite and too quickly at the soma. Much better fits were obtained by assuming R_m was lower in distal than in proximal regions.

Estimated parameter values from seven studies are given in table 10.1. The parameter values show some variability, but on average the C_m and R_a values are in line with those mentioned at the beginning of this chapter that were directly measured or calculated. The heterogeneity may reflect actual differences among cell types, differences in recording methods, problems with morphological reconstructions, or (except for the spinal cord study) uncertainty about appropriate compensation for dendritic spines.

Table 10.1
Passive electrotonic parameter value estimates from recent studies of seven different cell types

Study	Cell type	C_m ($\mu F/cm^2$)	R_a ($\Omega \cdot cm$)	R_m ($k\Omega \cdot cm^2$)
Trevelyan and Jack (2002)	Layer 2/3 cortical pyramidal (37°)	0.78–0.94	140–170	Soma shunt
Thurbon et al. (1998)	Spinal cord cells	2.4 ± 0.5	87 ± 22	5.3 ± 0.9
Roth and Hausser (2001)	Cerebellar Purkinje cells	0.77 ± 0.17	115 ± 20	122 ± 18
Stuart and Spruston (1998)	Layer 5 cortical pyramidal cells	1.1–1.5	70–100	$35 \rightarrow 5$ nonuniform
Major et al. (1994)	CA3 pyramidal cells	0.7–0.8	170–340	120–200
Golding et al. (2005)	CA1 pyramidal cells	1–2	139–218	$87 \rightarrow 20$ nonuniform
Chitwood et al. (1999)	Hippocampal interneurons	0.9 ± 0.3	Not available	61.9 ± 34.2

Parameter value ranges or means $\pm$ SD are given.

10.6 Considerations for Constructing Passive Cable Models

When one develops a passive cable model to study a specific phenomenon, there are several steps one should take and there are many places where one can go wrong. In this and the following section we discuss some of the issues, make some recommendations, and discuss some potential pitfalls. Much of what we will say is also relevant for models that include active membrane conductances that are discussed in the next chapter.

Choosing a Morphology

One of the first issues to be resolved is what to use to represent the morphology of a cell. Earlier we discussed the equivalent-cylinder model, but some of its key assumptions—that dendrites all end at the same electrotonic distance and that diameters at branch points satisfy the 3/2 rule—are often violated. A reduced model with a simplified morphology that better captures the essential morphological characteristics of a cell could be useful for network models where computation time is an issue. One such simplification is to reduce the dendritic tree into an unbranched "equivalent cable" with variable diameter (Clements and Redman, 1989; Fleshman et al., 1988). Dendrites from a morphological reconstruction are divided into small segments having an equal electrotonic length, ΔX (or equivalently, for fixed R_m and R_a, equal $\ell/d^{1/2}$). Then the diameter of the equivalent cable, d_{eq}, at electrotonic distance X_j ($X_j = \sum_{i=1}^{j} \Delta X$) is determined from the diameters of all dendrites present at that distance by $d_{\text{eq}}(X_j) = [\sum_i d_i(X_j)^{3/2}]^{2/3}$. This "equivalent cable" has approximately the same membrane area, input resistance, and time constant τ_0 as the fully branched structure, but the voltage transients are not identical (Rall et al., 1992).

The equivalent-cable model has been used to quickly estimate electrotonic parameter values from transients (Clements and Redman, 1989) and to collapse those parts of the dendritic tree not of interest for the question being modeled (Burke et al., 1994). It also provides a means to collapse subtrees in cells with more complicated structures for more efficient computation (Stratford et al., 1989).

With simplifications such as these, a cell may be represented with 10–40 compartments. However, if a simplified morphology is truly sufficient, then why has nature made dendritic trees so complicated? In recent years, a number of studies have shown that morphology plays an important role in the computations done by a cell (Hausser and Mel, 2003; Krichnar et al., 2002; Schaefer et al., 2003b; van Ooyen et al., 2002). With the advent of more powerful computers, computation time is not a major issue for models with detailed morphology, particularly passive models.

Detailed morphological reconstructions are becoming more and more available for a variety of cell types in public databases. The effort of anatomists to produce these data and to make them readily available is very much appreciated by the modeling community. Data that were maintained on web sites of individual labs are now being gathered more centrally. For example, http://neuromorpho.org, an archive maintained by G. A. Ascoli (2006), has collected reconstruction data for over a thousand cells from fifteen different laboratories. Much of this reconstruction data can be saved in NEURON and GENESIS formats. These morphological reconstructions provide an appropriate anatomical structure for the cell type without making any simplifying assumptions about morphology and should be used whenever possible.

Selecting Electrophysiological Data for Estimating Electrotonic Parameter Values

It is not enough to take a morphological reconstruction and use standard or typical values for the electrotonic parameters R_m, R_a, and C_m in a model. Values for these parameters must be fit to electrophysiological data so that the model not only has a representative morphological structure, but also produces representative electrophysiological responses. Ideally, one would like to have morphological and electrophysiological data from the same cell (and this is essential if the goal is to estimate actual values for electrotonic parameters, as discussed in the previous section), but these data are available in only a few labs, and morphology databases typically have no recordings from the reconstructed cells. There is a great need in the modeling community for a public database containing actual electrophysiological recordings with a number of repeated trials, even if the detailed morphology of such cells is not known.

Assuming electrophysiological data can be obtained, what type of data would be most useful for parameter fitting? Because we are discussing passive models, we first of all want our data to be free of the influence of voltage-dependent conductances. Brief current pulses are often used because they should not activate voltage-

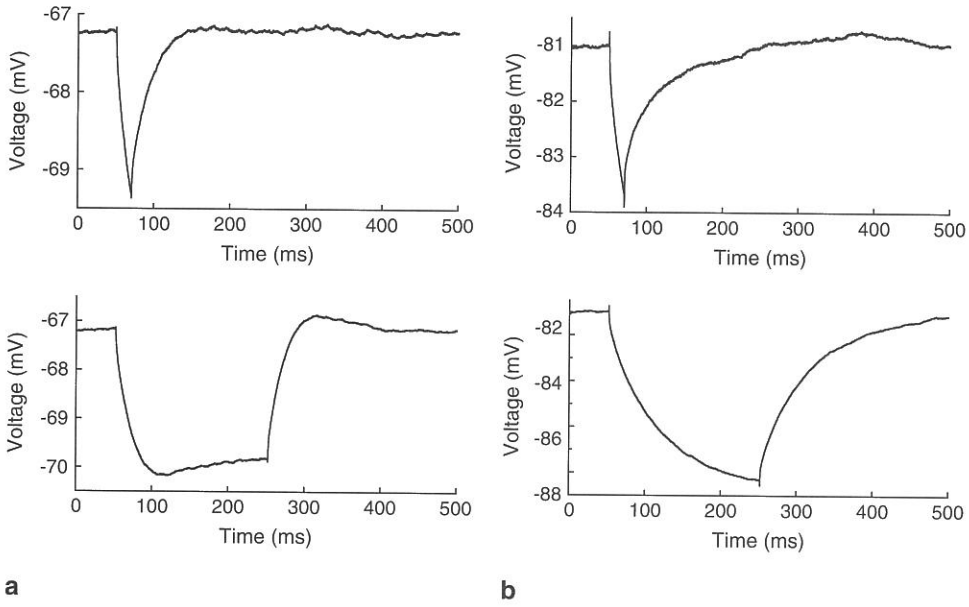

Figure 10.3
Experimental recordings in response to hyperpolarizing current pulses. Response to short (upper traces) and long (lower traces) hyperpolarizing current pulses from hippocampal CA1 pyramidal cells. (a) Cell in normal artificial cerebrospinal fluid (ACSF). (b) Cell with the H-channel blocker ZD-7288. The cell in ACSF shows the characteristic voltage sag in response to a long-duration current injection. The sag is eliminated in the other cell where the H-current is blocked.

dependent conductances. Weak hyperpolarizing and depolarizing current pulses can be used, and if we are fortunate, voltage changes with these currents will scale linearly with current amplitude. If not, then some cocktail of blockers of voltage-dependent conductances will have to be used. The voltage responses to short and long −50-pA current pulses injected into a CA1 hippocampal pyramidal cell are shown in figure 10.3a. The response shows the characteristic voltage sag seen in these cells that results from activation of the hyperpolarization-activated current, I_h. This current is blocked in another CA1 pyramidal cell by bath application of the H-channel blocker ZD-7288, as shown in figure 10.3b. The sag is gone and the voltage response is purely passive.

Second, we want to have voltage traces that provide sufficient information to estimate the electrotonic parameters. A long hyperpolarizing pulse will provide information about R_m and R_a, as well as input resistance, and the time course will provide information about R_m and C_m. A short hyperpolarizing pulse will provide information primarily about R_a and C_m, so both short and long current pulses should be used. In a passive system, it is not very useful to have data with current pulses of dif-

ferent amplitudes and the same duration except to check that the system is indeed linear and to catch possible problems caused by experimental noise, because no new information will be obtained. Recordings at sites different from the soma can provide useful information, particularly if the sites of the inputs are known and the morphology and electrophysiology come from the same cell, as noted earlier (Stuart and Spruston, 1998; Golding et al., 2005; Roth and Hausser, 2001). Other types of data, such as more complicated waveforms, direct current field stimulation (Svirskis et al., 2001), or impedance functions (Maltenfort and Hamm, 2004) may also be useful.

Compensation for Dendritic Spines

Many neuron types receive synaptic inputs on dendritic spines. A neuron can have many thousands of dendritic spines whose combined membrane area can be half the total membrane area of the cell. It is tedious to model every single spine explicitly and more tedious and generally not practical to measure spine dimensions for every spine on a cell (but see White and Rock, 1980). However, if one merely assigns standard values for R_m, C_m, and R_a to a morphological model without including spines or otherwise compensating for them, then the model will not provide an appropriate electrotonic structure. Input resistance will be overestimated and the results will not be representative.

There are two methods used in models to compensate for dendritic spines. The first is to increase C_m and reduce R_m according to total membrane area with spines included compared with total membrane area without spines (W. R. Holmes, 1989). For example, if the inclusion of spines on a dendritic segment increases total membrane area by 33%, then these spines can be included implicitly by multiplying C_m by 1.33 and dividing R_m by 1.33. Because spine density may not be the same in different parts of the cell, it is necessary to determine spine area and change R_m and C_m separately for each dendrite. A second method is to keep R_m and C_m the same on each dendrite, but increase the length and diameter of the dendrite to account for the extra membrane contributed by spines, but in such a way as to keep intracellular resistance (equivalently, length divided by diameter squared) the same (Stratford et al., 1989). In the earlier example where spines increase total membrane area by 33%, we let $F = 1.33$ and then multiply length by $F^{2/3}$ and diameter by $F^{1/3}$. It is quite simple to implement either of these two methods in simulation scripts.

These two methods for including spines work identically in passive models, but have very different implications for models with voltage-dependent conductances in dendrites. The first method, where R_m and C_m are changed, compensates for spines with passive membranes, whereas the second method, where length and diameter are changed, assumes that spines have the same densities of voltage-dependent conductances as the dendrite. The process of collapsing spines that are not passive and do not have the same voltage-dependent properties as the dendrite to which they

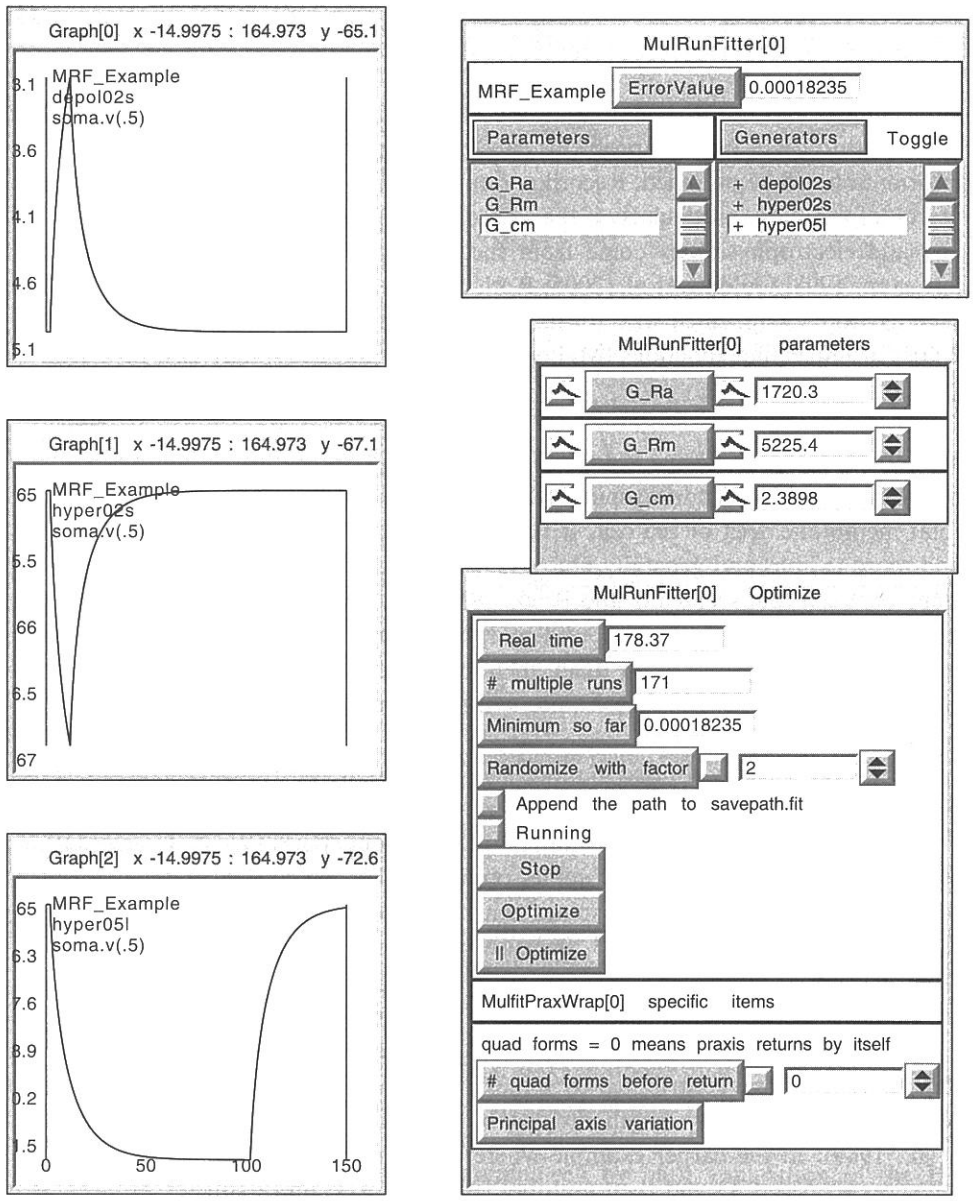

Figure 10.4
Local minima and sensitivity issues during the parameter search. Example using NEURON's multiple-run fitter. The "neuron" has a simple Y-branched apical dendrite, a basilar dendrite, and an axon (all passive). Spines were included on apical dendrites. The "experimental data" were generated with $R_m = 12{,}000$ Ωcm^2, $R_a = 160$ Ωcm, and $C_m = 1.0$ $\mu\text{F/cm}^2$ for all compartments. The fitter converged to these values with error 9e–10. However, with different starting values, there was convergence to a local minimum with parameter values that gave a very good-looking fit (fit and target traces overlap; parameter values and error shown in the figure). R_m, R_a, C_m combinations of (15,629, 53.296, 0.65739) or (14,811, 72.23, 0.72814) have low error and provide good fits visually, but were not considered final solutions by the fitter. The files to run this example are available on the book website at http://www.compneuro.org.

are attached is relatively straightforward, but requires that one be careful in the implementation.

Estimation of Electrotonic Parameter Values

After choosing a morphology for the model, selecting electrophysiological data and arranging to compensate for spines, if necessary, the next step is to fit electrotonic parameter values to make the model responses match the data. There are several ways this can be done. One method that we have found particularly useful, and which has been used by several groups, as noted earlier, is the multiple-run fitter available in the NEURON simulator (figure 10.4). NEURON uses the principal axis method (PRAXIS), a variant of the conjugate gradient method developed by Brent (1976), by default; see Shen et al. (1999). Chapter 2 discusses other parameter search methods that can be added to the NEURON multiple-run fitter or else used independently.

10.7 Problems, Pitfalls, and Recommendations

Problems with Morphological Reconstruction Data

The use of morphological reconstructions for modeling studies is recommended because a fixed and accurate morphology greatly reduces the number of degrees of freedom for the model. However, despite the enormous effort that is put into doing a morphological reconstruction and the improvements in reconstruction methodology through the years, the fact remains that precise morphological measurements are difficult to obtain (see chapter 8). Process diameters in particular are very difficult to measure accurately because many diameters are near the limit of resolution of the light microscope. Diameter measurements given in databases rarely have more than one digit of precision. Other potential problems are tissue shrinkage, artificial compression of tissue, and the difficulty of reconstructing lengths accurately in the z-axis direction as processes are followed from one plane of focus to another. Recent studies have analyzed reconstructions of the same cell type compiled by different labs (Ambros-Ingerson and Holmes, 2005; Scorcioni et al., 2004; Szilagy and De Schutter, 2004) and have found that morphological parameters such as total dendritic length, membrane area, and volume were similar among cells reconstructed in the same lab but were very different among different labs. This variability in measurements among labs is unlikely to be explained by differences in animal strain or age.

The variability in reconstructed measurements has consequences for estimates of electrotonic parameters. Recall that R_m is the membrane resistivity of a unit area of membrane in units of ohms times square centimeter, C_m is membrane capacitance per unit of area in units of microfaradays per square centimeter, and R_a is axial

resistivity through a unit cross-sectional area per unit of length in units of ohms times centimeter. Consequently, if the reconstruction diameters are uniformly off by a factor of x, then the fitting procedure will return estimates of R_m, C_m, and R_a equal to the actual R_m multiplied by x, the actual C_m divided by x, and the actual R_a multiplied by x^2. If reconstruction lengths are uniformly off by a factor y, then the fitting procedure will return estimates of R_m, C_m, and R_a equal to the actual R_m multiplied by y, the actual C_m divided by y, and the actual R_a divided by y. R_a estimates are particularly vulnerable to error because of the x^2 dependence of its estimate on diameter and the fact that diameter is difficult to measure precisely. Despite the consequences of reconstruction errors for the electrotonic parameter estimates, reconstructed morphologies should still be used in the models. They provide a characteristic anatomical structure of the cell type being studied, and issues with reconstructions can be overcome with parameter fitting, as discussed next.

It Is Essential to Fit Parameter Values with Data

If one blindly uses standard values for R_m, C_m, and R_a in models based on reconstruction data, the results may not be representative for the cell type being studied. Even if the morphological data and the electrophysiological data come from the same cell and the morphological reconstruction is perfect, parameter estimation is still necessary for two reasons. First, although we know ranges of values for the electrotonic parameters, the "standard" values are not known precisely enough that one can confidently say that a model with such values will produce representative results. Second, even if the dendrites are reconstructed perfectly, it is unlikely that the number of dendritic spines or the total spine area is known with much precision. Parameter fitting will still be needed to account for dendritic spines.

Some models may be based on morphological data obtained from a database and electrophysiological data obtained from a different cell. The assumption is that the morphology chosen is typical and provides an appropriate structure for the cell and that the electrophysiological data are also typical. Here parameter fitting is necessary to compensate for (1) reconstruction issues, (2) an unknown number of spines, and (3) the fact that the two types of data come from different cells. Parameter fitting can make the morphological cell model electrotonically equivalent to the experimental cell (W. R. Holmes et al., 2006). Clearly, there is heterogeneity among cell types, and the morphology and cell responses of the reconstructed cell and the experimental cell may in fact be different. However, the morphological reconstruction provides a basic anatomical structure that is common for the cell type, and with fitted electrotonic parameter values, a model based on this reconstruction will provide representative responses for that cell type. This is really what we want even though the actual electrotonic parameter values in the model may not be typical or standard values.

Local Minima, Uniqueness, and Sensitivity Problems

Issues associated with parameter fitting are discussed in detail in chapter 2. It is not clear how often the problem of local minima appears when fitting passive models, but in our experience this has not been much of an issue when there are suitable bounds on the parameter space. In the very few cases where we have seen convergence to multiple solutions, the fitting error has clearly indicated the better solution. However, finding local minima in the simple example in figure 10.4 proved to be much easier than with real data. For example, with starting values of 100, 1,200, and 1 for R_a, R_m, and C_m, the method converges to $R_a = 1720.3$, $R_m = 5225.4$, and $C_m = 2.3898$. The model with these parameter values appears to overlap the "experimental" traces visually, as shown in figure 10.4. The error is very small, although it is orders of magnitude larger than the error with the "true" values. In situations like this, it is helpful to set physiological bounds on parameter values, but even then the method may sometimes get stuck on one of the bounds. It is advisable to try several different starting value combinations. The issue of nonuniqueness of parameter fits is discussed in chapter 12, section 3. For passive models, the fitting procedure described typically assumes that R_m, R_a, and C_m are uniform, but this does not have to be the case. It is likely that equally good (or better—Stuart and Spruston, 1998; Golding et al., 2005) solutions can be obtained if this assumption is relaxed and some functional form is used to describe how the values of these parameters change with distance from the soma. If these parameters are uniform, morphology provides a significant constraint limiting nonuniqueness. For example, in the equivalent-cylinder model values of L, R_N, and τ do not fix R_m, R_a, and C_m uniquely unless length and diameter are also specified. For more complex models, morphology plus experimental voltage traces appear to fix uniform R_m, R_a, and C_m values uniquely, but this has not been proven.

A larger problem is sensitivity. When the example in figure 10.4 is run, solutions that do not look bad visually appear long before convergence. If the fitter is stopped before convergence at one of these not-so-bad solutions, the parameter values may be significantly different from the "true" or final values. Experimental data contain noise, and there is no guarantee that noise will not cause very different parameter values to appear as the final solution (Major et al., 1994). If noise is truly random, then use of multiple sets of experimental data with different protocols might minimize this problem.

Recommendations for Modeling

Ideally one should try to get a morphological reconstruction and electrophysiological data from the same cell. Failing that, morphology can be obtained from a public database and electrophysiological data for the same cell type can be obtained

separately, but these two types of data should be matched for the same strain of animal at the same age. Passive electrotonic parameters in the model should be fit to match multiple voltage traces from the experimental cell, to make the modeled cell electrotonically similar to the experimental cell. Blind use of standard values for electrotonic parameters is not likely to yield representative results. Because of heterogeneity within a cell type in both morphological reconstructions and electrophysiological data, modeling studies should use multiple morphologies and multiple sets of experimental data; results generated from just one cell morphology and one set of experimental data should not be considered robust.

Acknowledgments

I would like to thank Jose Ambros-Ingerson for comments and suggestions on this chapter and Larry Grover for the experimental data shown in figure 10.3.